Supporting Information

Removal of Iron, Manganese, Cadmium, and Nickel Ions Using Brewers' Spent Grain

Karina Haro Carrasco, Egon Götz Höfgen, Dominik Brunner, Konstantin B. L. Borchert, Berthold Reis, Christine Steinbach, Martin Mayer, Simona Schwarz, Karl Glas and Dana Schwarz

Table of content

1 Results

1.1 Characterization of BSG

1.1.1 Gas sorption analysis

1.1.1.1 Nitrogen sorption isotherms

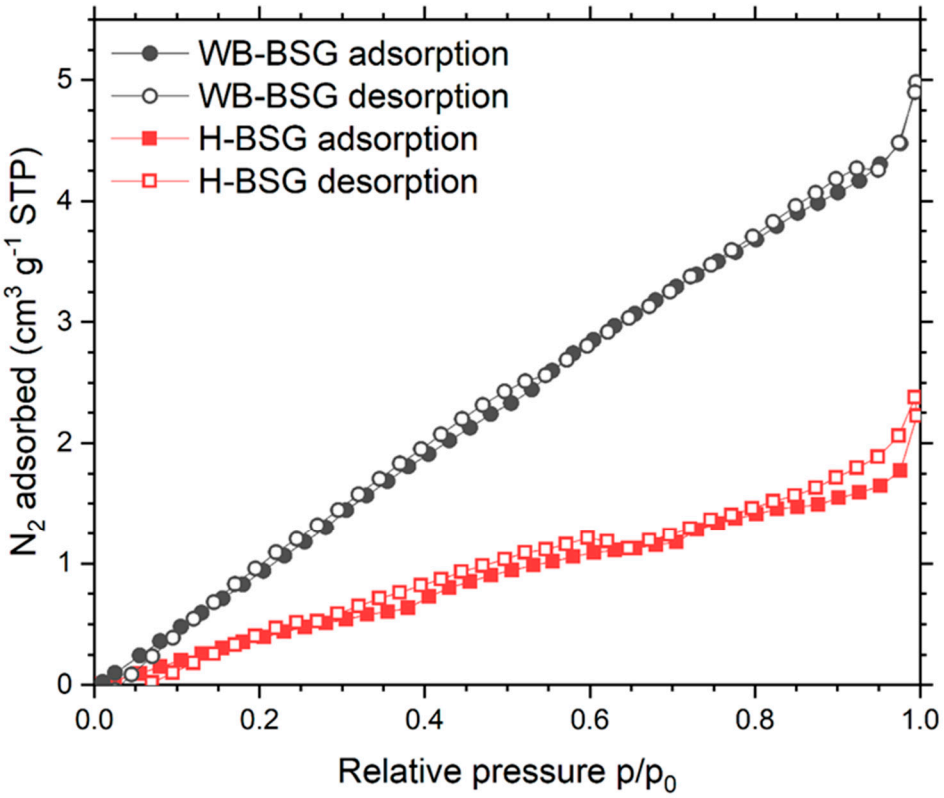

Figure S1. Nitrogen sorption isotherm at 77 K of WB-BSG (grey) and H-BSG (red), desorption denoted by hollow symbols.

1.1.1.2 *Carbondioxide sorption isotherms*

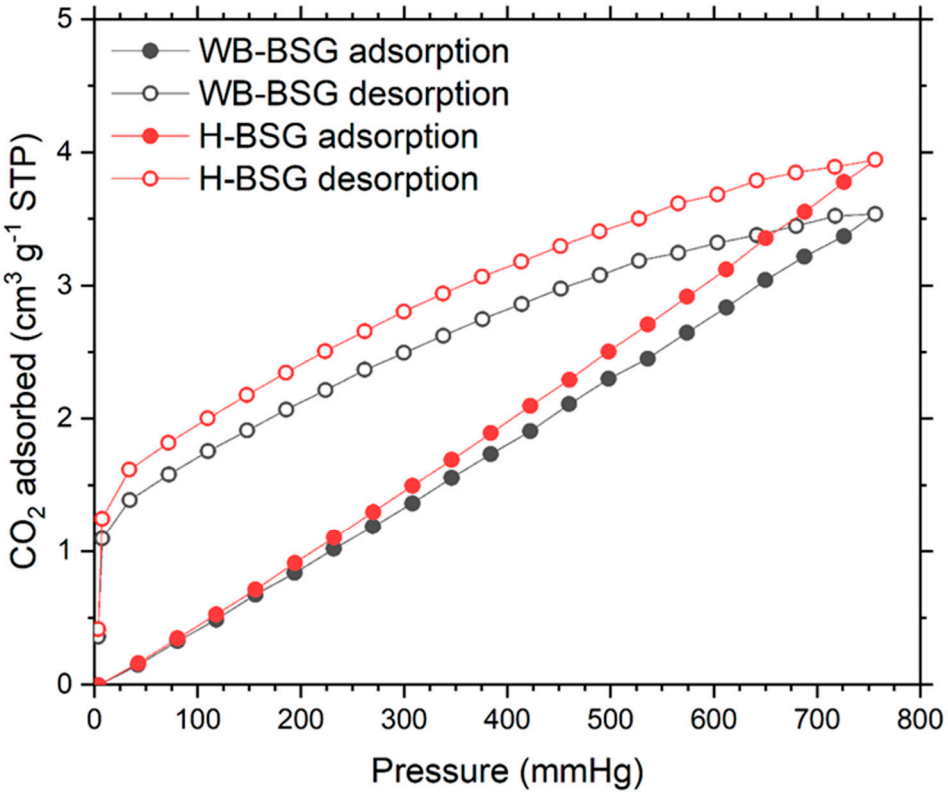

Figure S2. CO_2 sorption isotherm at 273 K of WB-BSG (grey) and H-BSG (red), desorption denoted by hollow symbols.

1.1.2 Charge Density

Table S1. Measurements of charge densities (q) at pH values 3, 5.5, and 7 of H-BSG and WB-BSG. V_{used} Volumes of Polyelectrolyte (poly(sodium ethylenesulfonate) (PES-Na) solution or poly(diallyldimethylammonium chloride) (PDADMAC)) used until point of zero charge.

Sample	Initial pH_0	mass (g)	Potential	V_{used} (mL)	mean V_{used}(mL)	c (mmol/L)	q (µeq/g)
WB-BSG	**3**	0.1	+	0.0526	0.0543	(+) 0.005	**(+) 0.54**
		0.1	+	0.0559			
	5.5	0.1	–	0.1082	0.1089	(–) 0.011	**(–) 1.09**
		0.1	–	0.1096			
	7	0.1	–	0.2384	0.2455	(–) 0.025	**(–) 2.46**
		0.1	–	0.2526			
H-BSG	**3**	0.1	+	0.0690	0.0637	(+) 0.006	**(+) 0.64**
		0.1	+	0.0583			
	5.5	0.1	–	0.4408	0.4203	(–) 0.042	**(–) 4.20**
		0.1	–	0.3997			
	7	0.1	–	0.7444	0.7671	(–) 0.077	**(–) 7.67**
		0.1	–	0.7898			

1.1.3 Moisture analysis

Table S2. Moisture analysis performed at 110 °C until mass was constant.

Sample	Moisture (%)	Solids content (%)
WB-BSG	2.82	97.18
H-BSG	1.08	98.92

1.1.4 ICP-OES analysis of elemental composition of BSG

Table S3. Relative elemental content of BSG and comparison to literature.

Study	**This study**		**[1]**	**[2]**	**[3] *mean concentrations**
Method	**ICP- OES**		**ICP-OES**	**XRF**	**ICP-AAS**
Sample	**WB-BSG, industrial brewery**	**H-BSG, industrial brewery**	**Pilsner BSG, craft brewery,**	**BSG, industrial brewery**	**fresh BSG, Carlsberg Malaysia,**
Cu (mg/kg)	19.33	37.98	-	-	2.5*
Mn (mg/kg)	95.89	33.27	41	44.4 (as MnO_2)	9.5*
Zn (mg/kg)	103	77.21	139	107 (as ZnO)	-
Fe (mg/kg)	166	121	240	217 (as Fe_2O_3)	63.5*
Si (mg/kg)	392	530	791	-	242*
K (mg/kg)	411	321	849	247 (as K_2O)	-
Na (mg/kg)	707	1373	166	103 (as Na_2O)	60.5*
S (mg/kg)	2265	2640	-	-	8.5*
Mg (mg/kg)	2456	1921	2509	122 (as MgO)	688*
Ca (mg/kg)	4939	2821	2669	595 (as CaO)	1038*
P (mg/kg)	6793	4703	5861	-	1977*
Se (mg/kg)	n.a.	n.a.	-	-	6*

1.1.5 SEM-EDX analysis of BSG prior adsorption

1.1.5.1 SEM-EDX analysis of H-BSG

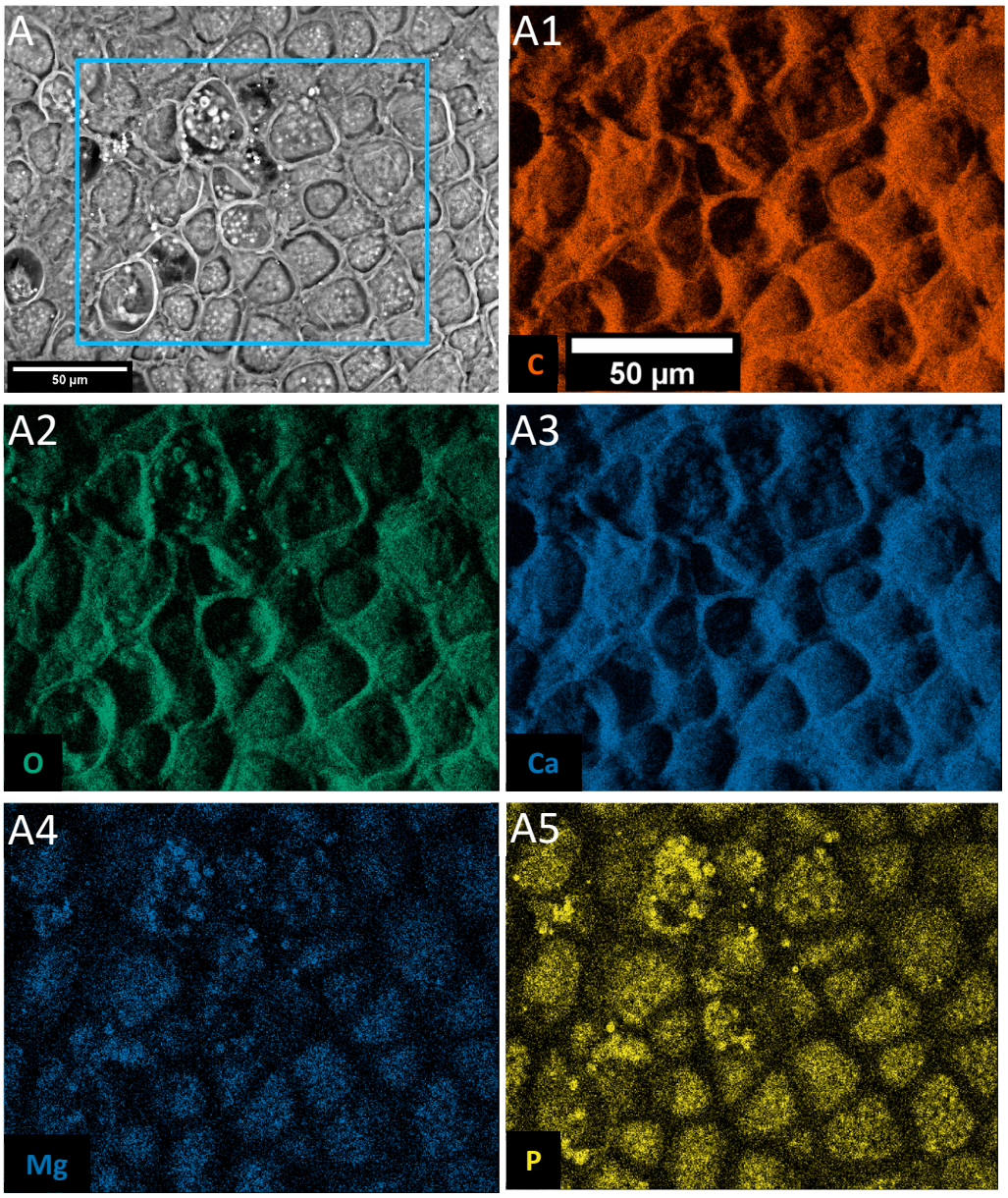

Figure S3. H-BSG Map A prior adsorption SEM-EDX elemental mapping, all scale bars = 50 µm. Subfigure A SEM micrograph with mapped area (Map A) highlighted as blue rectangles. Subfigures: A1 carbon mapping; A2 Oxygen mapping; A3 Calcium mapping; A4 Magnesium mapping; A5 Phosphorus mapping; data summarized in Table S4.

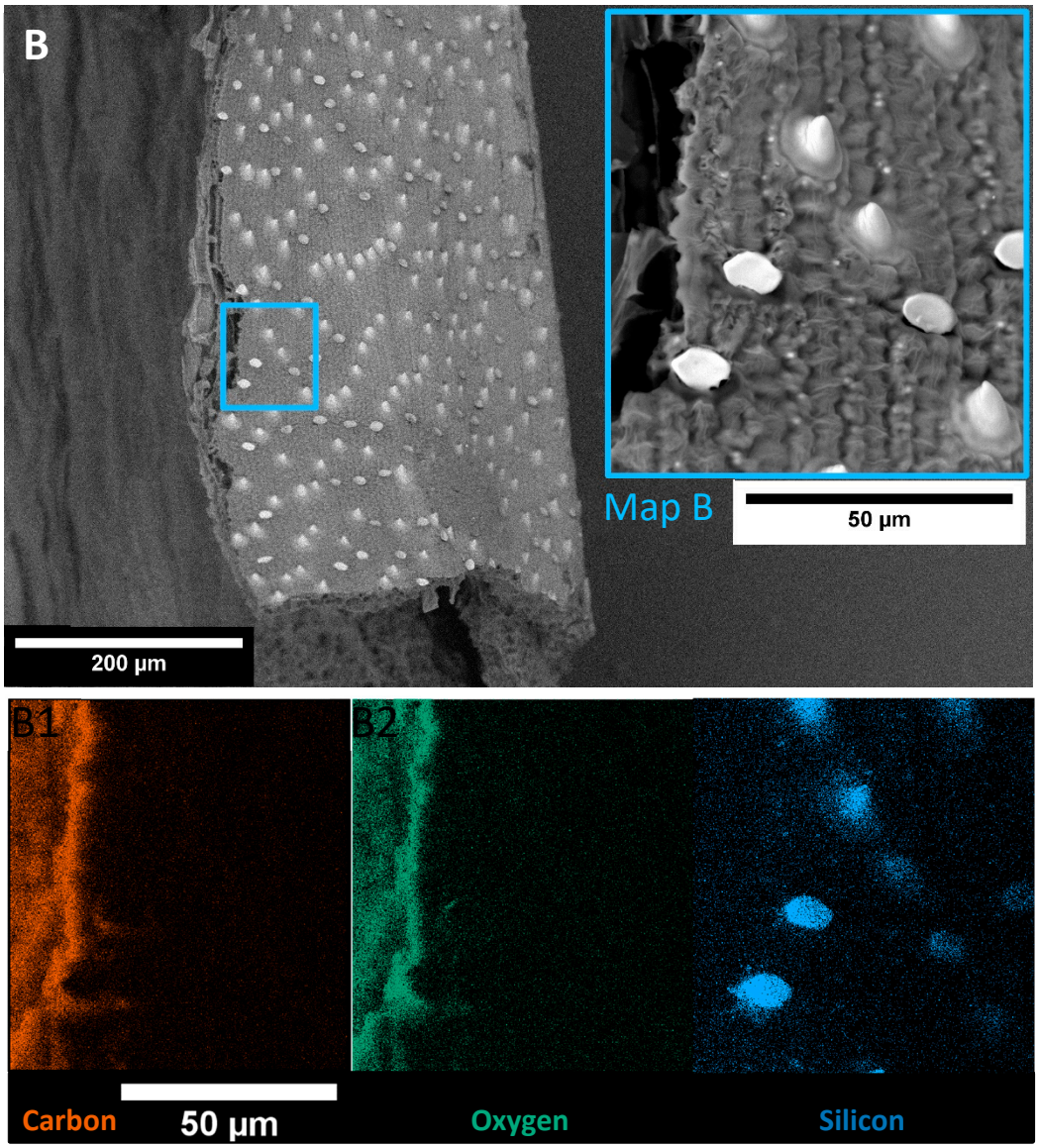

Figure S4. H-BSG Map B prior adsorption SEM-EDX analysis. Subfigure B showing SEM micrograph, area mapped as Map B highlighted as blue rectangles and magnified as insert. Subfigure B1 carbon mapping; subfigure B2 Oxygen mapping; subfigure B3 Silicon mapping; data summarized in Table S4.

Table S4. Elemental concentration as percentages detected in two areas of H-BSG prior adsorption. Selected areas are Map A of Figure S4 and Map B of Figure S5.

% atomic concentration	**Map A Figure S4**	**Map B Figure S5**
Carbon	68.611	65.037
Oxygen	29.526	33.456
Silicon	-	1.507
Phosphorous	0.964	-
Calcium	0.508	-
Magnesium	0.391	-
% weight concentration	**Map A Figure S4**	**Map B Figure S5**
Carbon	60.761	57.487
Oxygen	34.835	39.397
Silicon	-	3.116
Phosphorous	2.202	-
Calcium	1.502	-
Magnesium	0.701	-

1.1.5.2 SEM-EDX analysis of WB-BSG

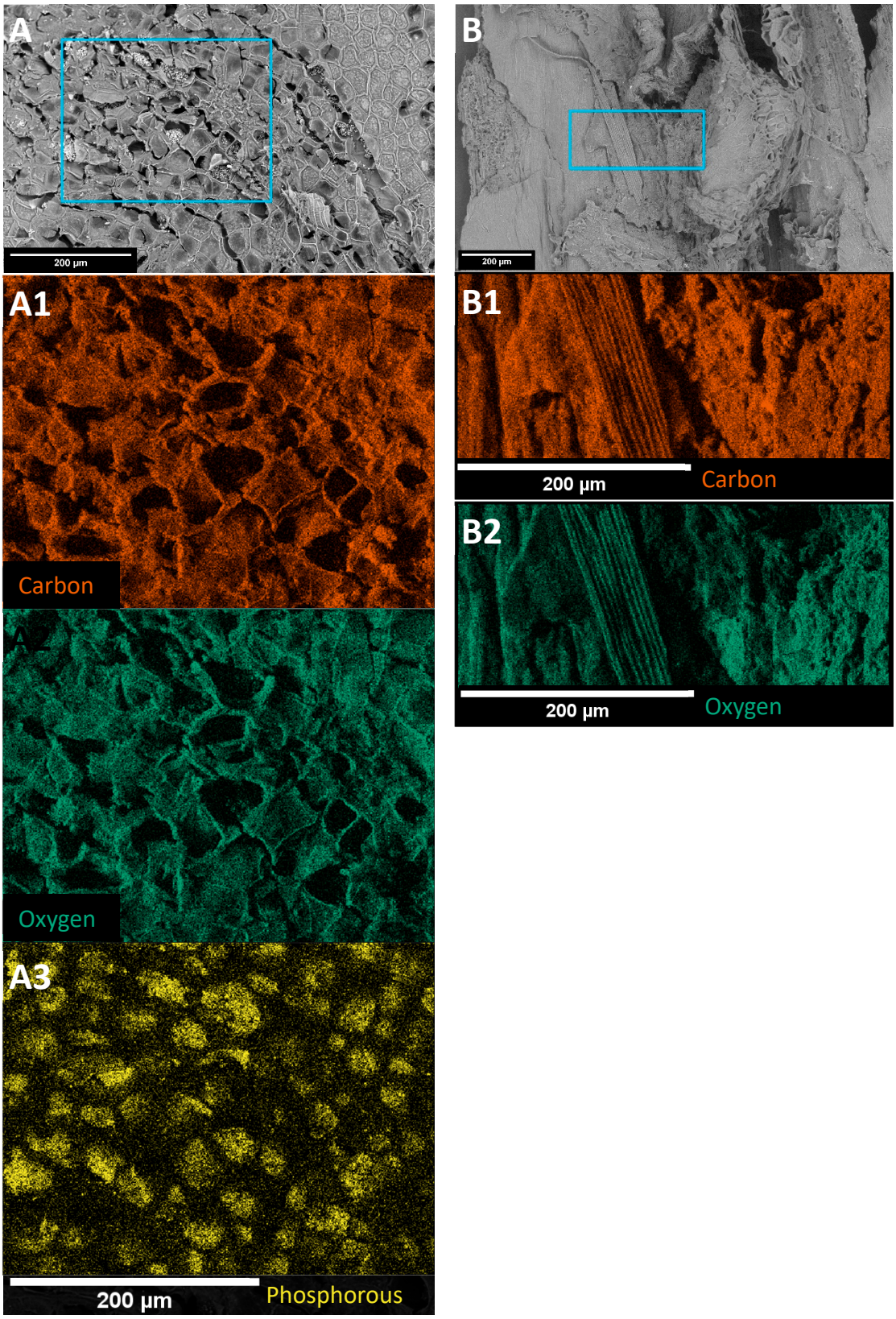

Figure S5. SEM-EDX elemental mapping of WB-BSG pre adsorption, all scale bars = 200 µm. Subfigures A and B are SEM micrographs, blue rectangles highlighted mapped areas Map A and Map B. Subfigure X1 carbon mapping; Subfigure X2 Oxygen mapping; Subfigure X3 Phosphorus mapping; data summarized in Table S5.

Table S5. Elemental concentration as percentages detected in two areas of WB-BSG prior adsorption. Selected areas Map A and B shown in Figure S6.

% atomic concentration	**Map A**	**Map B**
Carbon	58.557	60.916
Oxygen	39.401	39.084
Phosphorous	0.95	-
Calcium	0.804	-
Magnesium	0.288	-
% weight concentration	**Map A**	**Map B**
Carbon	50.15	53.916
Oxygen	44.955	46.084
Phosphorous	2.098	-
Calcium	2.298	-
Magnesium	0.5	-

1.2 Adsorption experiments

1.2.1 Kinetic adsorption experiments

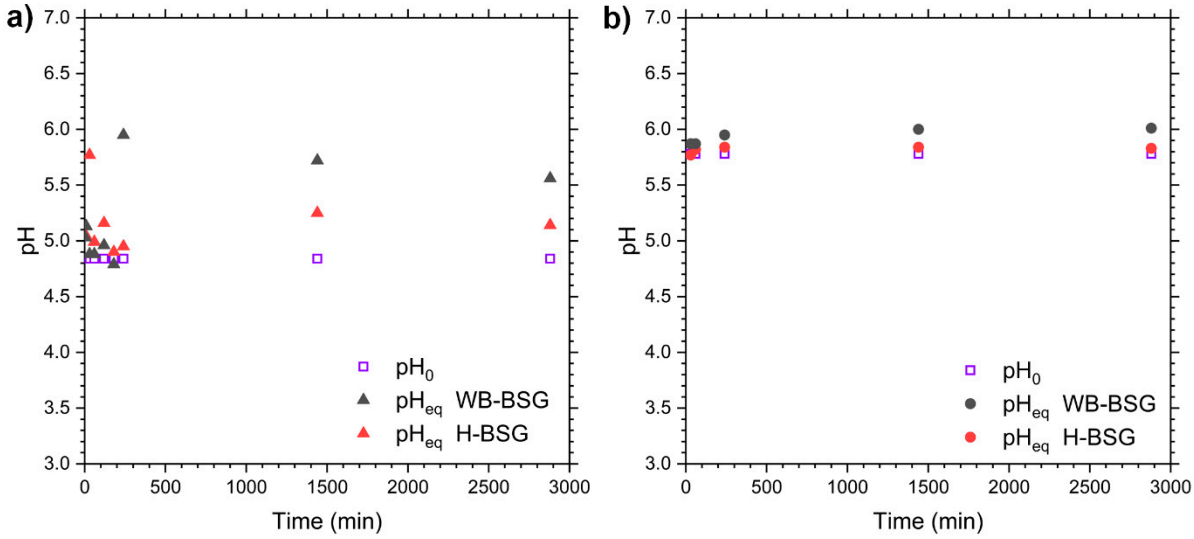

Figure S6. pH values before (pH_0) and after (pH_{eq}) adsorption in kinetic experiments with a) $FeSO_4$ and b) $MnSO_4$ solutions onto H-BSG and WB-BSG. From batch experiments with c_0 = 0.36 mmol/L $Fe^{2+/3+}$ or Mn^{2+}, a BSG dosage of 3.33 g/L, stirred at r.t. and measured at respective times.

Table S6. Parameters for linear fitting shown in Figure 6.

Parameters	**$Fe^{2+/3+}$**		**Mn^{2+}**	
$f(x) = ax + C$	**H-BSG**	**WB-BSG**	**H-BSG**	**WB-BSG**
Part I				
a	0.044	0.0372	0.0169	0.0116
C	0.0112	0.0158	0.0179	0.0275
R^2	0.93	0.95	0.92	0.67
Part II				
a	0.00374	0.00467	0.00159	0.00535
C	0.0857	0.0812	0.0335	0.0353
R^2	0.38	0.36	0.77	0.93

1.2.2 Sorption of $FeSO_4$ and $MnSO_4$

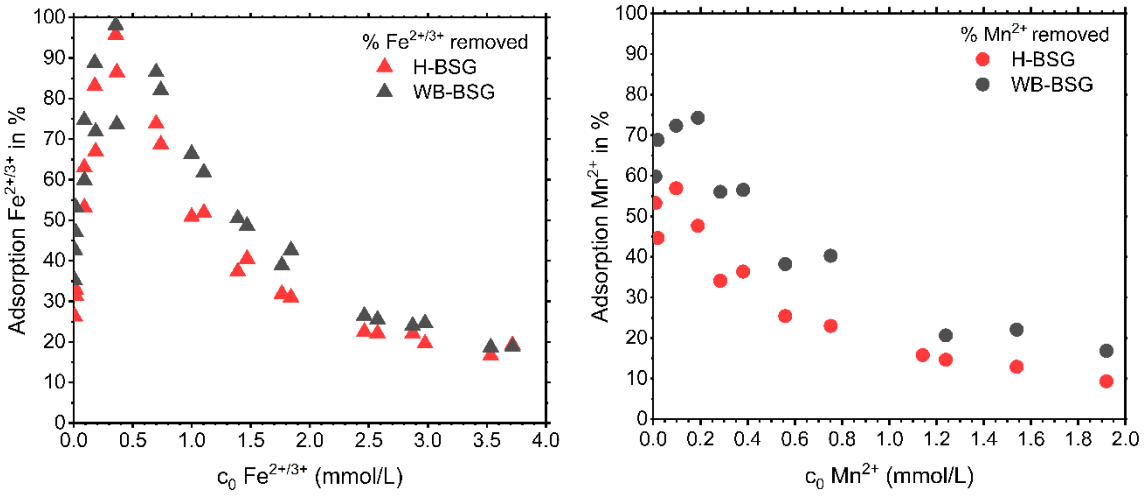

Figure S7. Removal rate for $Fe^{2+/3+}$ and Mn^{2+} ions by adsorption onto H-BSG and WB-BSG, obtained from batch experiments with constant BSG dosage (3.33 g/L) and varying initial concentration of $FeSO_4$ or $MnSO_4$ for 24 h at r.t..

1.2.3 pH values of the batch sorption experiments for $FeSO_4$ and $MnSO_4$

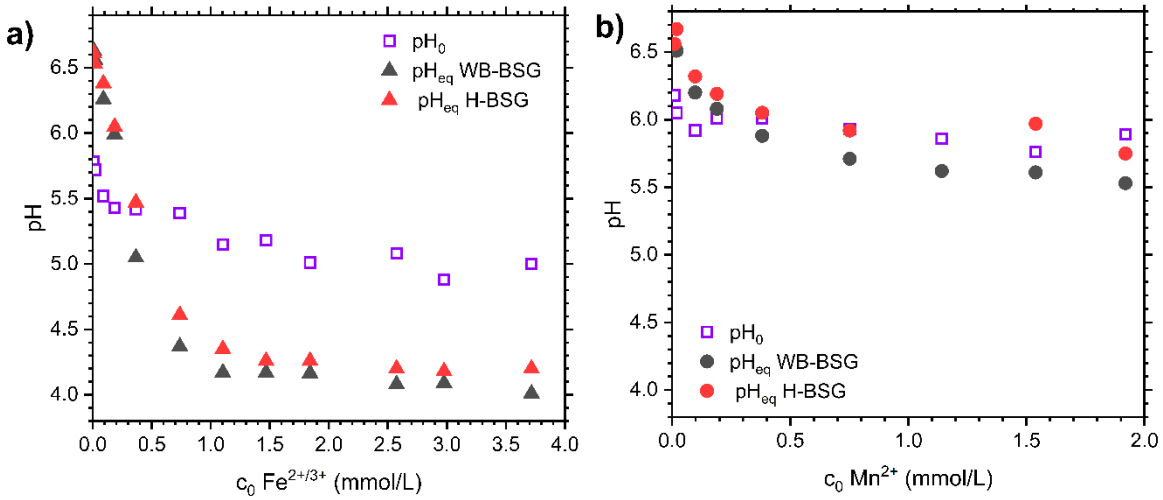

Figure S8. Changes of pH values throughout adsorption isotherm experiments with a) $FeSO_4$ and b) $MnSO_4$ solutions onto H-BSG and WB-BSG in batch experiments with constant dosage of adsorber material (3.33 g/L), varying initial concentrations $FeSO_4$, pH not adjusted 24 h, r.t..

1.2.4 Sorption isotherms of $FeSO_4$ with different fitting models

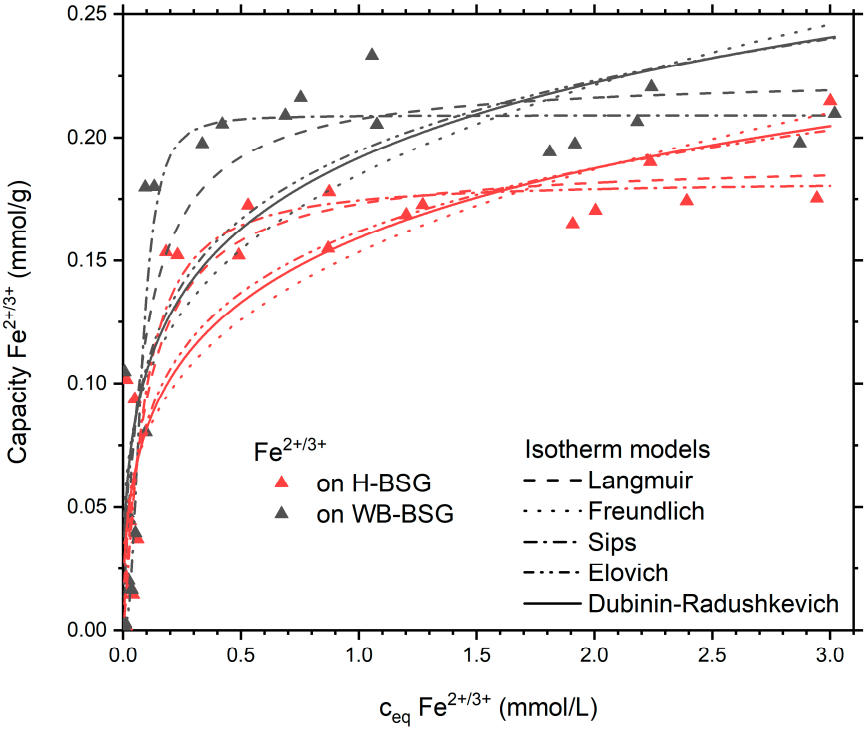

Figure S9. Curve fitting of different isotherm models onto $Fe^{2+/3+}$ ion adsorption onto H-BSG and WB-BSG in batch experiment with constant dosage of adsorber material (3.33 g/L), varying initial concentrations $FeSO_4$, pH not adjusted 24 h, r.t..

1.2.5 Sorption isotherms of $MnSO_4$ with different fitting models

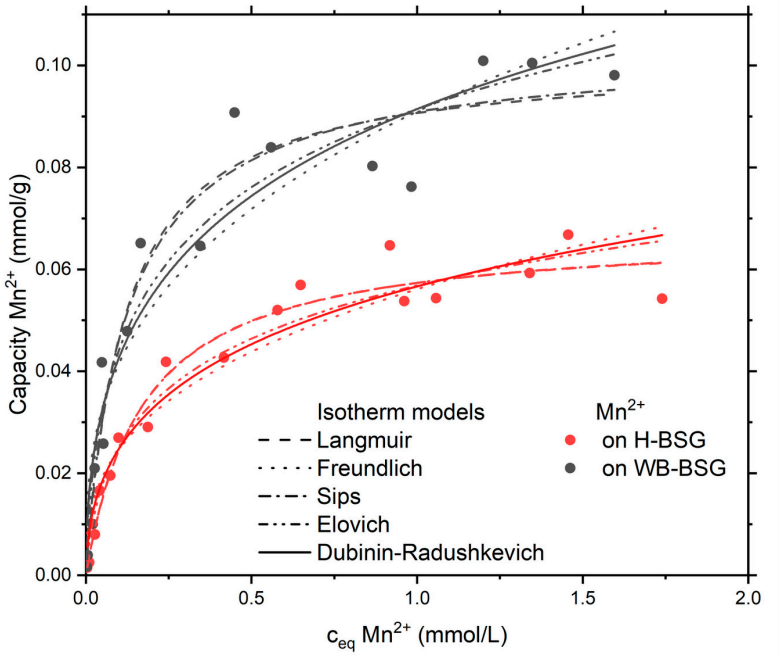

Figure S10. Curve fitting of different isotherm models onto Mn^{2+} ion adsorption onto H-BSG and WB-BSG in batch experiment with constant dosage of adsorber material (3.33 g/L), varying initial concentrations $MnSO_4$, pH not adjusted 24 h, r.t..

1.2.6 Comparison of isotherm model fitting

Table S7. Fitting parameters for different adsorption isotherm models. Data from batch experiments; constant dosage of H-BSG or WB-BSG 3.33 g/L, varying initial concentrations $FeSO_4$ or $MnSO_4$, pH not adjusted, 24 h, r.t,.

Adsorption parameters	$Fe^{2+/3+}$		Mn^{2+}	
	H-BSG	**WB-BSG**	**H-BSG**	**WB-BSG**
Langmuir				
$Q_{m,L}$ (mmol/g)	0.191 ± 0.01	0.226 ± 0.013	0.0674 ± 0,003	0.101 ± 0.005
K_L (L/mmol)	9.585 ± 2.625	11.443 ± 3.280	5.718 ± 0,981	8.489 ± 1.731
R^2	0.884	0.869	0.964	0.951
ΔG° (kJ/mol)	-22.72	-23.15	-21.44	-22.41
Freundlich				
n	3.494 ± 0.563	3.852 ± 0.719	2.805 ± 0.350	2.937 ± 0.383
K_F $(L/mmol)^{1/n}$	0.153 ± 0.009	0.185 ± 0.012	0.0561 ± 0.002	0.0909 ± 0.004
R^2	0.791	0.729	0.910	0.890
Sips				
$Q_{m,S}$ (mmol/g)	0.182 ± 0.011	0.209 ± 0.009	0.0678 ± 0.006	0.104 ± 0.011
K_S $(L/mmol)^n$	22.145 ± 24.266	786.822 ± 1935,065	5.471 ± 3.133	6.793 ± 4.889
n	1.280 ± 0.351	2.6196 ± 0.962	0.98428 ± 0.191	0.93208 ± 0.212
R^2	0.888	0.894	0.964	0.952
Elovich				
$Q_{m,E}$ (mmol/g)	0.0474 ± 0.008	0.0514 ± 0.010	0.0213 ± 0.003	0.0301 ± 0.004
K_E	103.734 ± 73.78	166.266 ± 140,872	38.598 ± 17.400	63.712 ± 31.637
R^2	0.844	0.795	0.945	0.942
Dubinin-Radushkevich				
$Q_{m,DR}$ (mmol/g)	0.376 ± 0.052	0.417 ± 0.063	0.163 ± 0.021	0.244 ± 0.033
β $(10^{-9}\ mol^2/J^2)$	2.931 ± 0.445	2.649 ± 0.462	3.616 ± 0.394	3.342 ± 0.389
R^2	0.824	0.773	0.934	0.927
E_{ads} (kJ/mol)	13.06 ± 0.99	13.74 ± 1.20	11.76 ± 0.64	12.23 ± 0.71

1.2.7 SEM-EDX Analysis of BSG after adsorption of iron ions

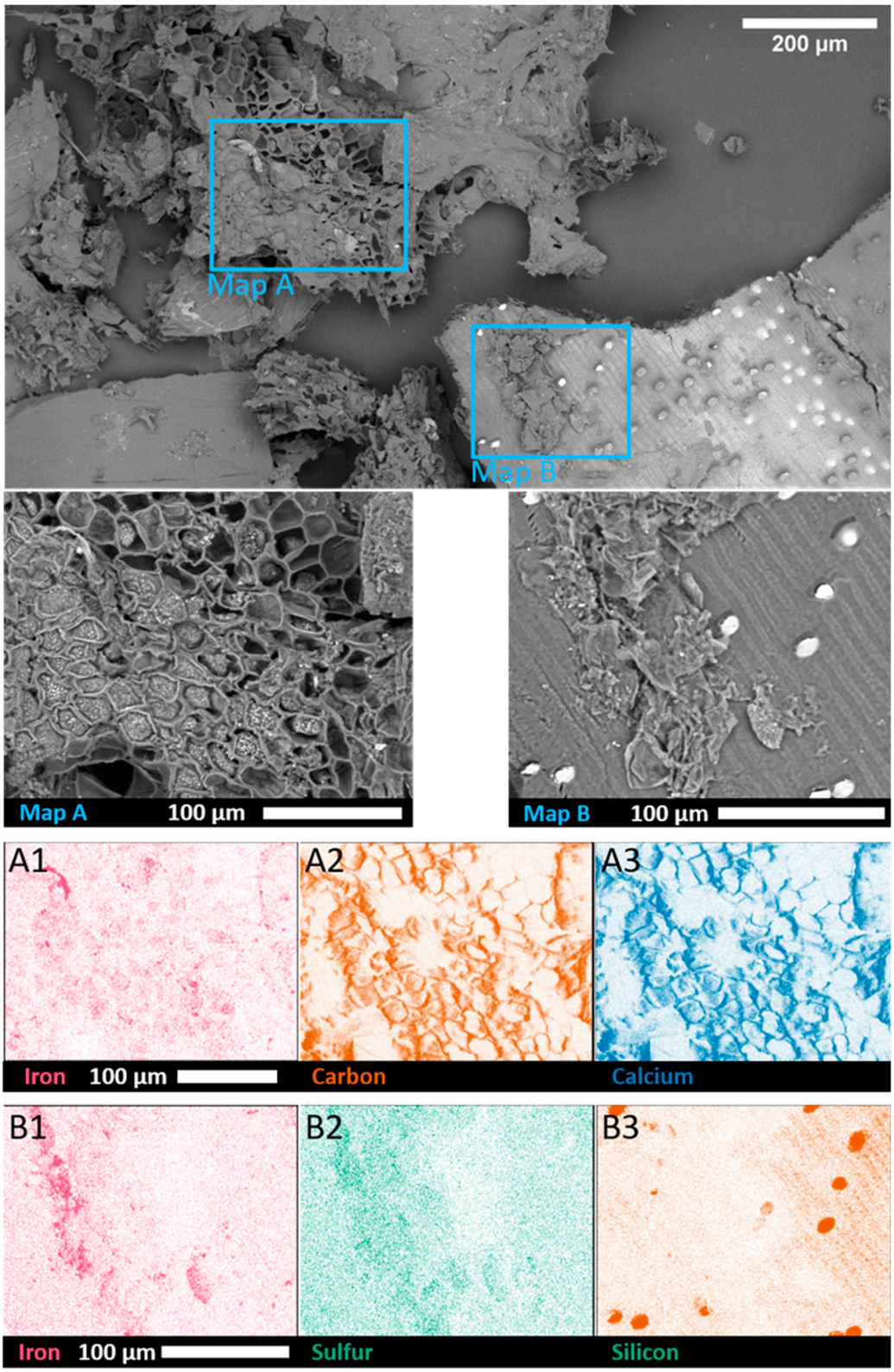

Figure S11. SEM-EDX elemental mapping of H-BSG after adsorption in batch experiments with $FeSO_4$ (2.68 mmol/L), 24 h at 23 °C. Top: regions selected for mapping highlighted as blue rectangles, map A and map B shown below. All subfigure scale bars represent 100 µm. Subfigure: Selected element mappings A1 and B1 iron; A2 carbon, B2 sulfur; A3 calcium; B3 silico; data summarized in Table S8.

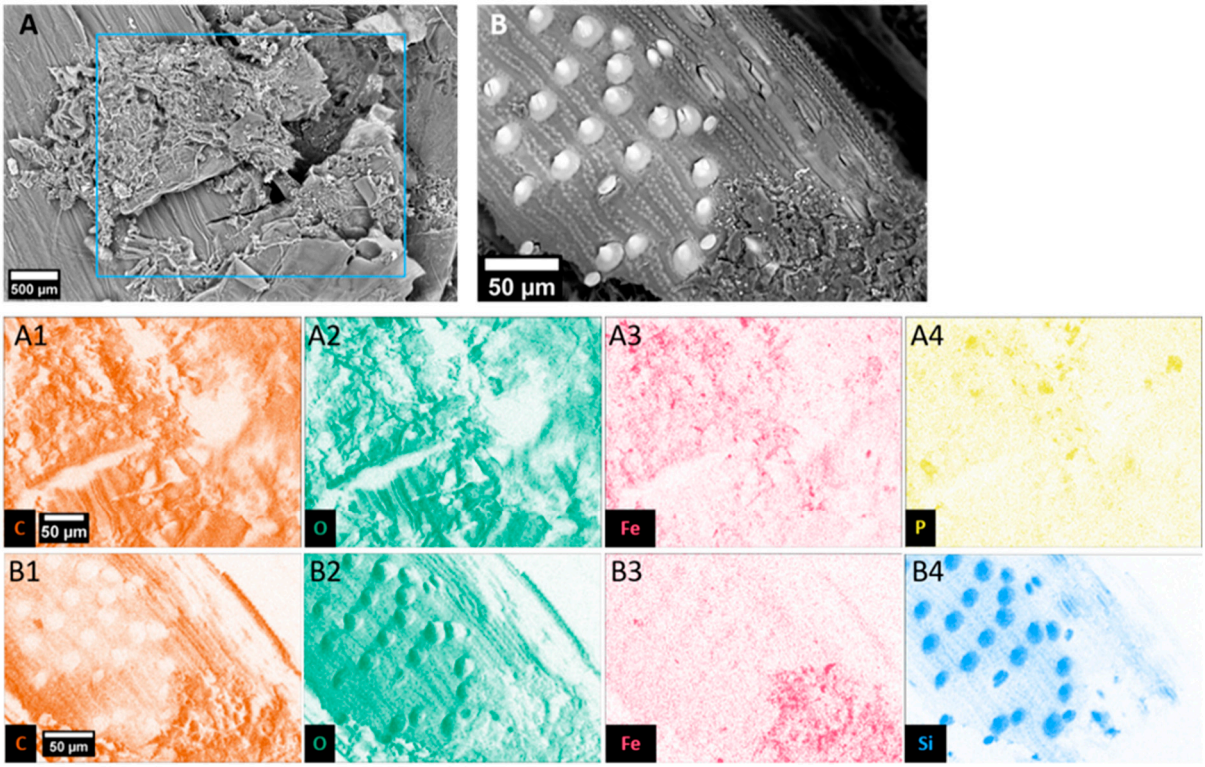

Figure S12. SEM-EDX elemental mapping of WB-BSG after adsorption in batch experiments with $FeSO_4$ (2.68 mmol/L), 24 h at 23 °C, all EDX scale bars = 50 µm. Subfigures A and B are SEM micrographs, blue rectangles in A highlights mapped area Map A. Subfigures show selected element mappings: A1 and B1 carbon; A2 and B2 oxygen; A3 and B3 iron; A4 phosphorus; B4 silicon; data summarized in Table S8.

Table S8. Elemental concentration as percentages detected on BSG surface after adsorption in batch experiments with $FeSO_4$ (2.68 mmol/L), 24 h at 23 °C. Investigated in two areas (map A and map B) of H-BSG Figure S10 and WB-BSG (Figure S11).

	H-BSG (Figure S10)		**WB-BSG (Figure S11)**	
% atomic concentration	**Map A**	**Map B**	**Map A**	**Map B**
Carbon	66.896	61.556	61.601	54.700
Oxygen	30.968	37.171	37.754	41.418
Phosphorus	0.858	0.089	0.224	-
Calcium	0.175	-	-	-
Iron	1.103	0.271	0.422	0.154
Sulphur	-	0.129	-	-
Silicon	-	0.784	-	3.728
% weight concentration	**Map A**	**Map B**	**Map A**	**Map B**
Carbon	57.631	53.646	53.831	45.846
Oxygen	35.542	43.157	43.952	46.246
Phosphorus	1.908	0.200	0.504	-
Calcium	0.502	-	-	-
Iron	4.418	1.099	1.714	0.601
Sulphur	-	0.300	-	-
Silicon	-	1.598	-	7.307

1.2.8 SEM-EDX Analysis of BSG after adsorption of manganese ions

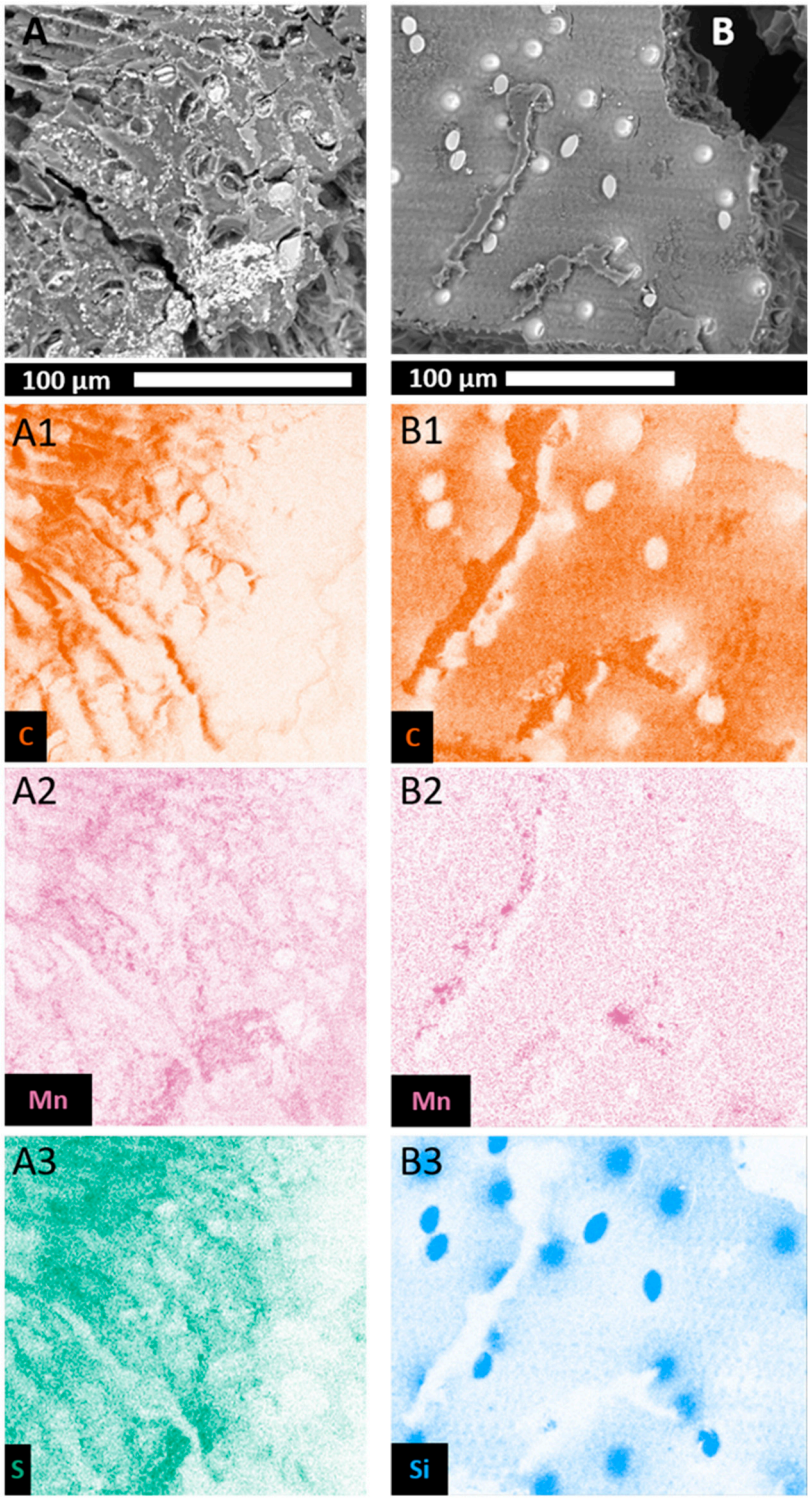

Figure S13. SEM-EDX elemental mapping of H-BSG after adsorption in batch experiments with $MnSO_4$ (2.91 mmol/L), 24 h at 23 °C, universal scale bars = 100 µm. Subfigures A and B are SEM micrographs of mapped areas. Subfigures show selected element mappings: A1 und B1 carbon; A2 und B2 manganese ; A3 sulphur; B3 silicon; data summarized in Table S9.

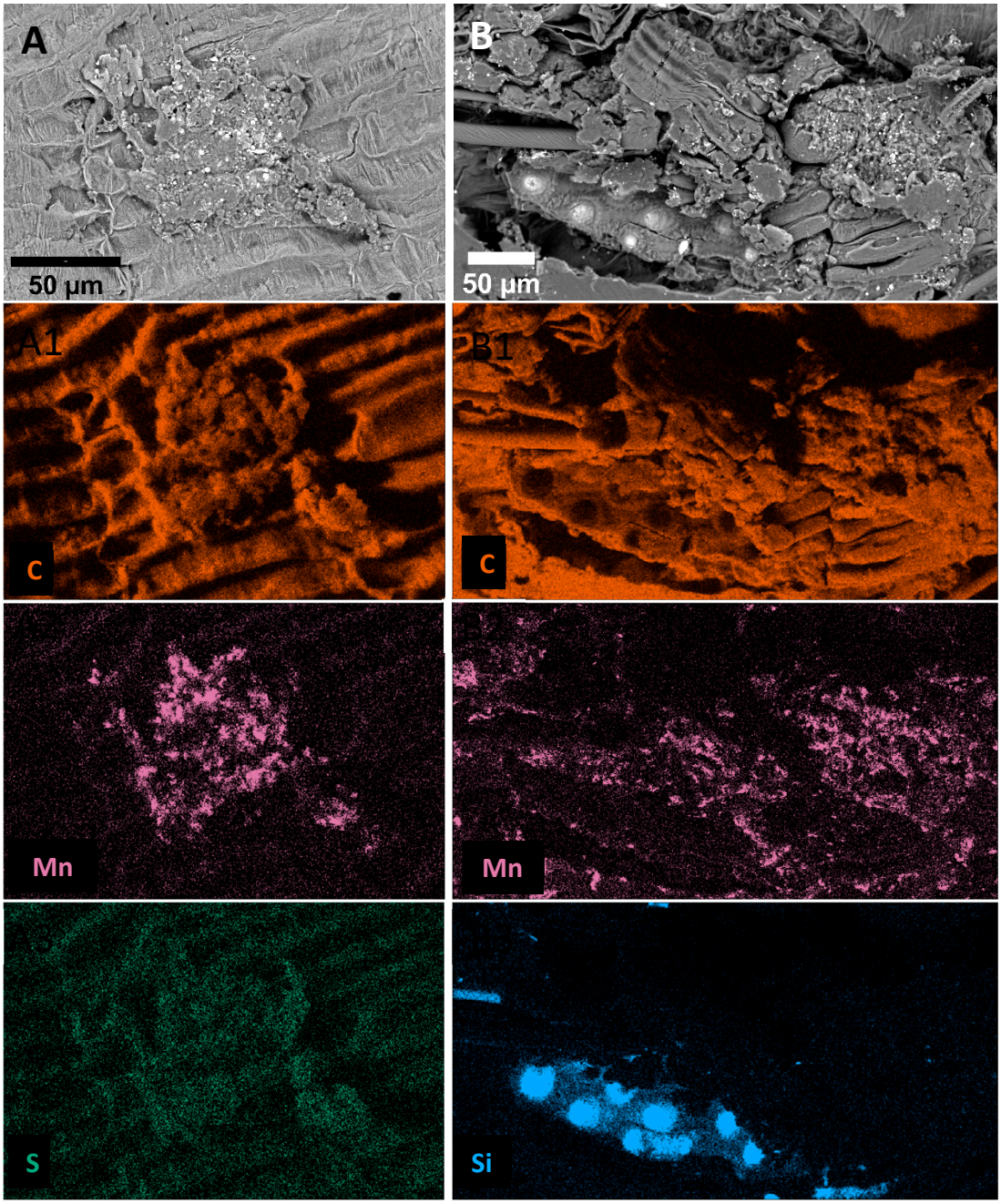

Figure S14. SEM-EDX elemental mapping of WB-BSG after adsorption in batch experiments with $MnSO_4$ (2.73 mmol/L), 24 h at 23 °C, universal scale bars = 50 µm. Subfigures A and B are SEM micrographs of mapped areas. Subfigures show selected element mappings: A1 und B1 carbon; A2 und B2 manganese; A3 sulphur; B3 silicon; data summarized in Table S9.

Table S9. Elemental concentration as percentages detected on BSG surface after adsorption in batch experiments with $MnSO_4$ (H-BSG: 2.91 mmol/L; WB-BSG 2.73 mmol/L), 24 h at 23 °C. Investigated in two areas (map A and map B) of H-BSG (Figure S12) and WB-BSG (Figure S13).

	H-BSG (Figure S12)		**WB-BSG (Figure S13)**	
% atomic concentration	**Map A**	**Map B**	**Map A**	**Map B**
Carbon	64.811	56.385	68.222	63.945
Oxygen	30.009	41.002	31.397	35.444
Silicon	0.584	2.561	-	0.486
Manganese	2.633	0.051	0.209	0.124
Sulphur	1.488	-	0.171	-
Phosphorus	0.289	-	-	-
Calcium	0.186	-	-	-
% weight concentration	**Map A**	**Map B**	**Map A**	**Map B**
Carbon	52.462	48.096	61.245	56.653
Oxygen	32.362	46.593	37.550	41.835
Silicon	1.106	5.110	-	1.008
Manganese	9.749	0.200	0.502	0.504
Sulphur	3.216	-	0.703	-
Phosphorus	0.603	-	-	-
Calcium	0.503	-	-	-

1.2.9 Adsorption with real water samples

Table S10. Initial concentrations c_0 of selected pollutants in 2 water samples from German surface waters and sorption efficiency by H-BSG and WB-BSG given as averages of six batches with standard deviation. Batch experiments performed with real water, 3.33 g/L dosage of H-BSG or WB-BSG for 24 h at r. t.

	Sample 1			**Sample 2**		
Parameter	c_0 mmol/L	Average sorption %		c_0 mmol/L	Average sorption %	
		H-BSG	WB-BSG		H-BSG	WB-BSG
Sulfate	18.850	1.6 ± 0.9	1.8 ± 1.1	3.958	3.9 ± 1.8	1.8 ± 4.5
$Fe^{2+/3+}$	0.005	98.9 ± 0.7	99.3 ± 1.1	1.612	97.5 ± 0.6	95.8 ± 0.9
Mn^{2+}	0.002	0	0	0.048	0.2±0.4	0.7 ± 0.7
Si	0.176	0	0	2.182	0.8 ± 0.9	1.3 ± 3.1
pH_0; av. pH_{eq}	6.98[1]	6.27[2]	6.3[2]	3.1[1]	3.18[2]	3.25[2]

[1] pH_0 in the respective surface water samples

[2] average (av.) pH_{eq} after sorption experiments

Figure S15. Exemplary photograph of the state of German surface waters in mine drainage regions (real water sample 2).

1.2.10 Adsorption with $NiSO_4$

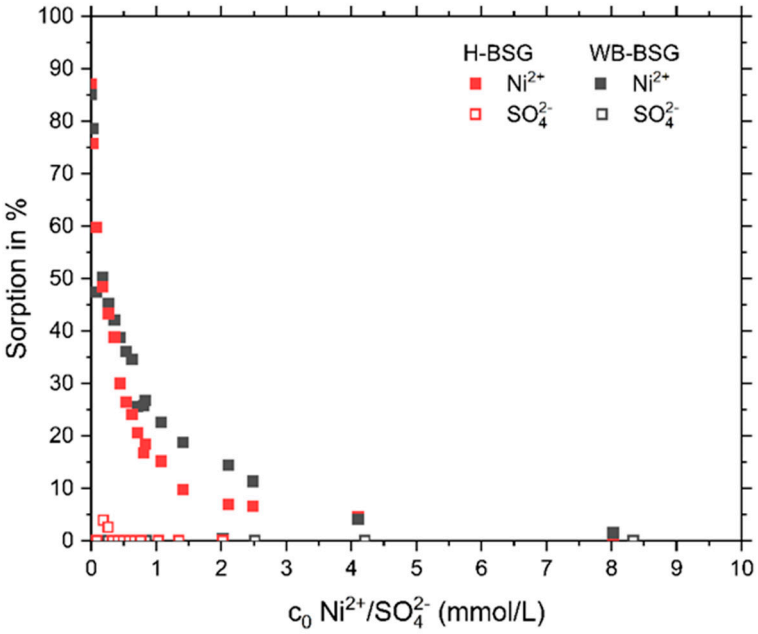

Figure S16. Adsorption in % for Ni^{2+} and SO_4^{2-} ions with H-BSG and WB-BSG, obtained from batch experiments and stirred for 24 h.

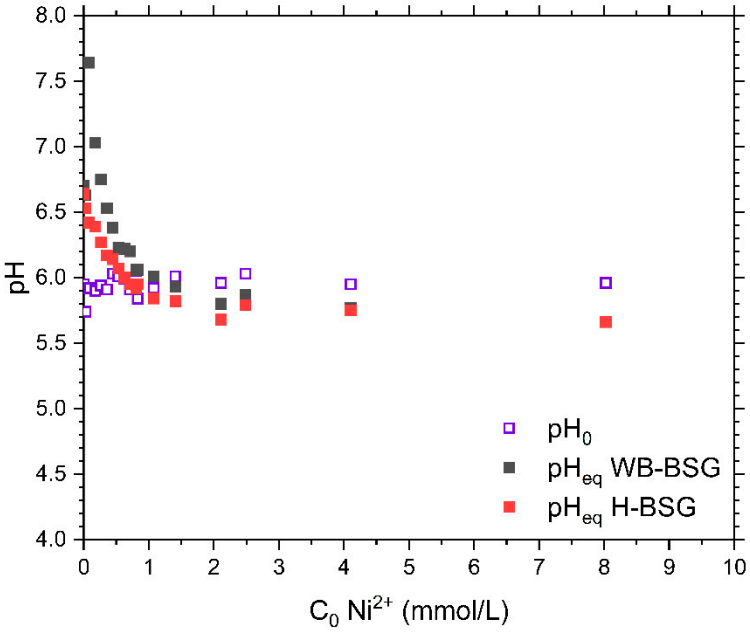

Figure S17. pH values before (pH_0) and after (pH_{eq}) for the adsorption of Ni^{2+} and SO_4^{2-} ions onto H-BSG and WB-BSG, obtained from batch experiments, stirred 24 h and pH not adjusted.

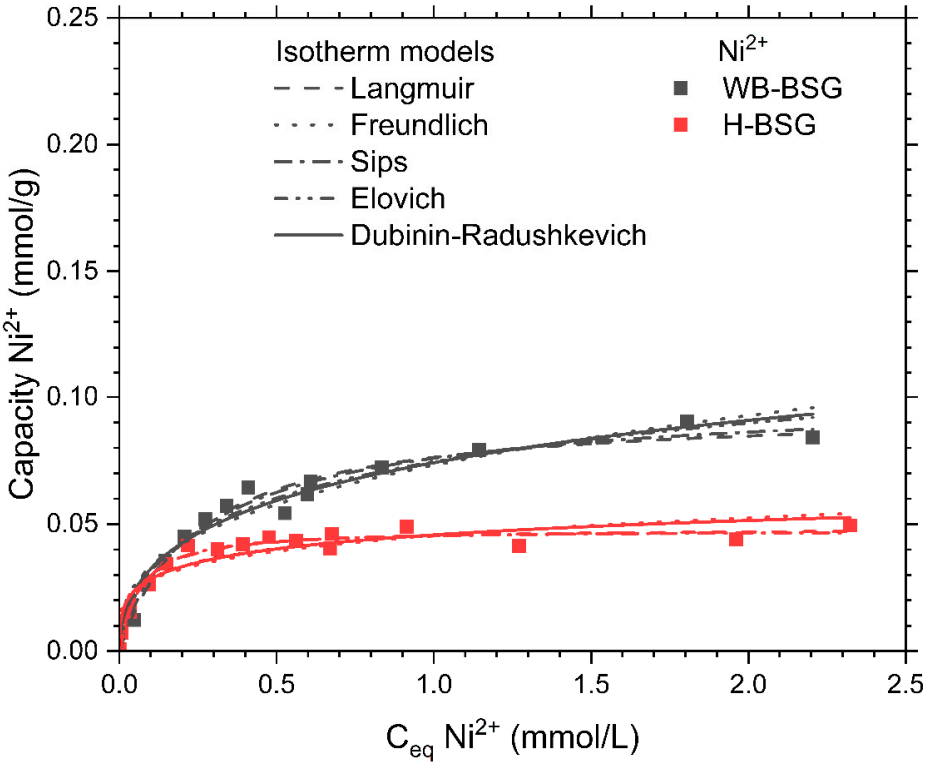

Figure S18. Curve fitting of different isotherm models onto Ni^{2+} adsorption onto H-BSG (red) and WB-BSG (grey) in batch experiment.

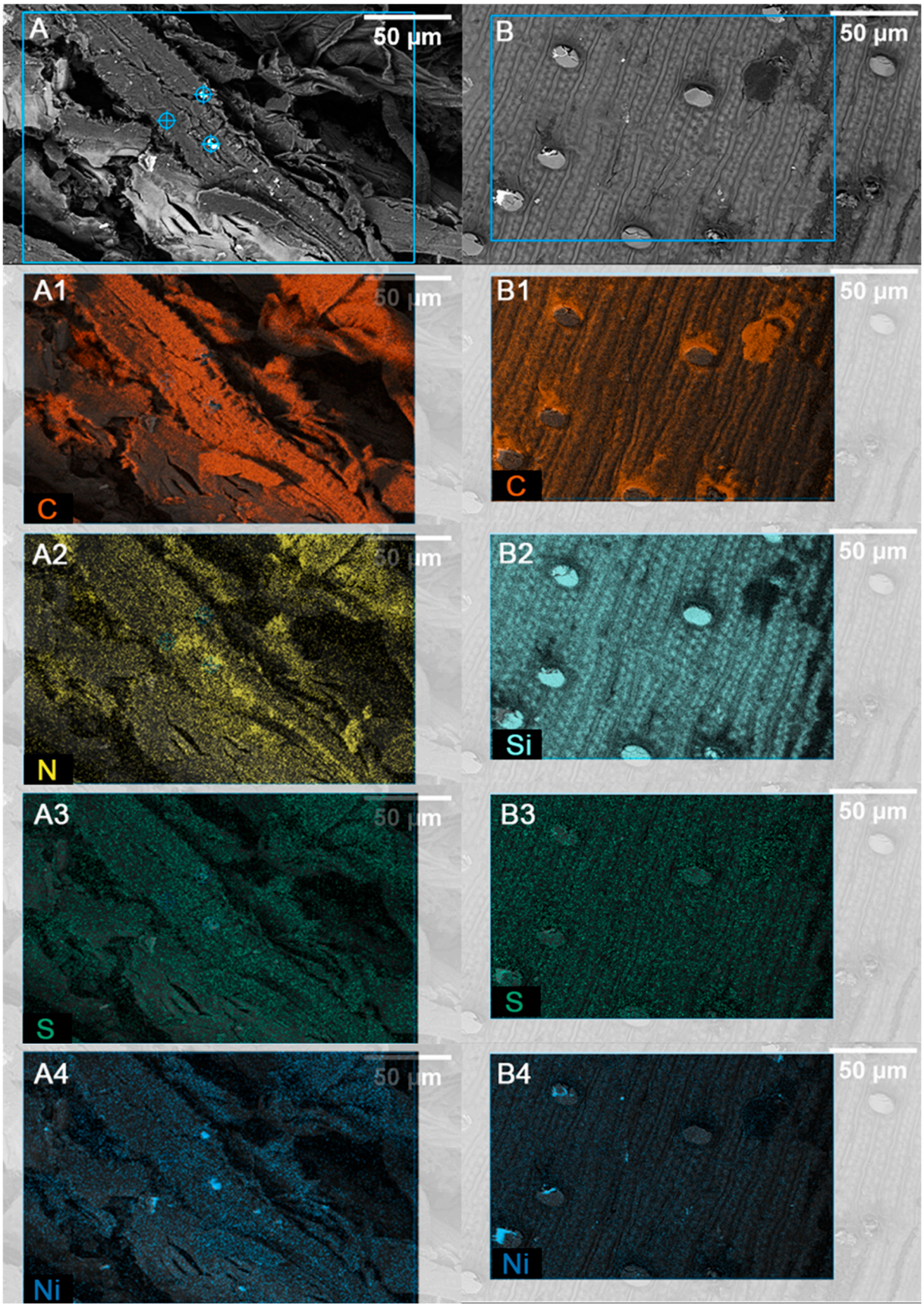

Figure S19. SEM-EDX elemental mapping of H-BSG after adsorption in batch experiments with $NiSO_4$ (2.5 mmol/L), 24 h at 23 °C, universal scale bars = 50 µm. Subfigures A and B are SEM micrographs of mapped areas. Subfigures show selected element mappings: A1 and B1 carbon; A2 nitrogen and B2 silicon; A3 and B3 sulphur and A4 and B4 nickel.

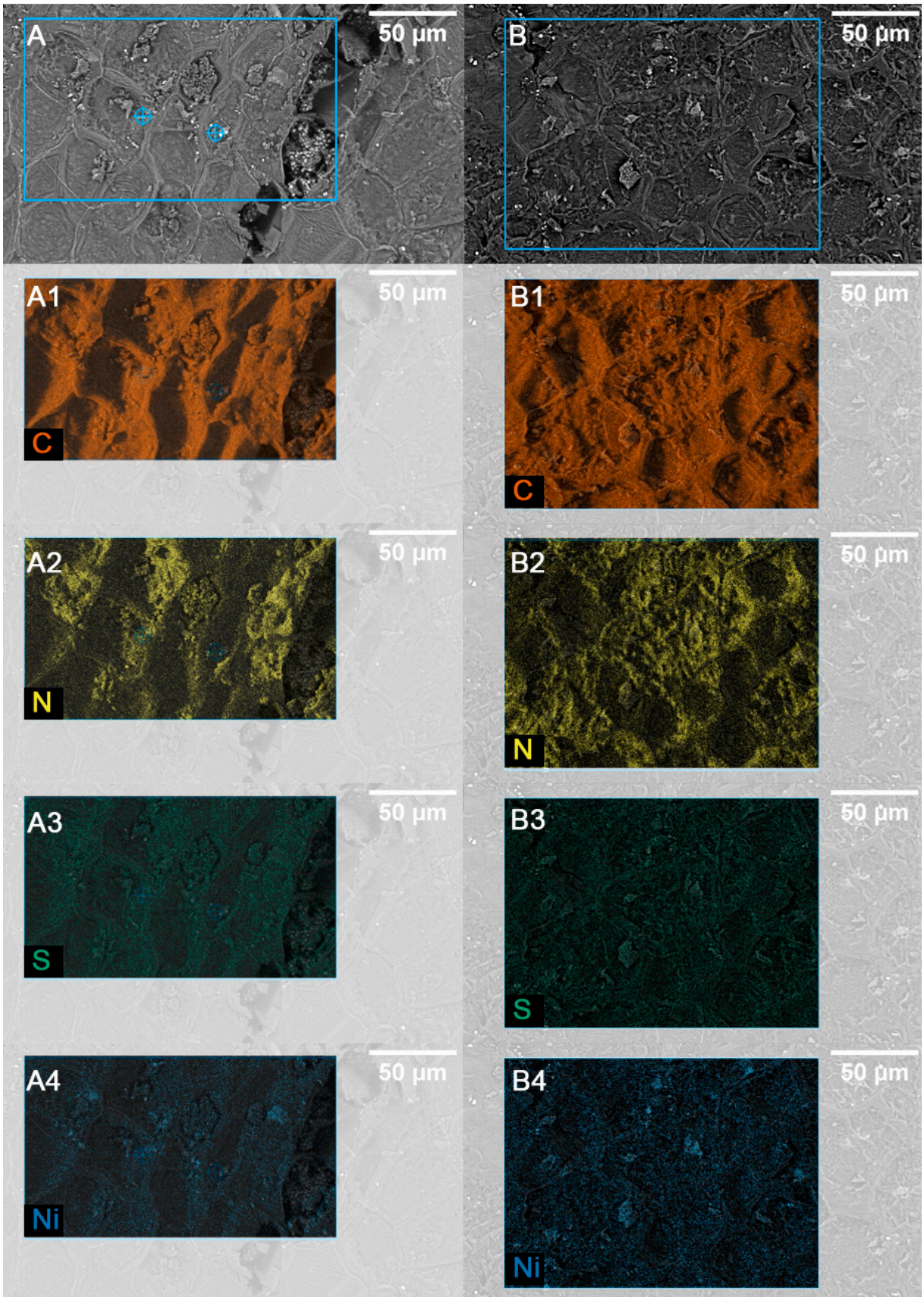

Figure S20. SEM-EDX elemental mapping of WB-BSG after adsorption in batch experiments with $NiSO_4$ (2.5 mmol/L), 24 h at 23 °C, universal scale bars = 50 µm. Subfigures A and B are SEM micrographs of mapped areas. Subfigures show selected element mappings: A1 and B1 carbon; A2 and B2 nitrogen, A3 and B3 sulphur and A4 and B4 nickel.

Table S11. Elemental concentration as percentages detected on BSG surface after adsorption in batch experiments with $NiSO_4$ (H-BSG: 2.5 mmol/L; WB-BSG 2.5 mmol/L), 24 h at 23 °C. Investigated in two areas (map A and map B) of H-BSG (**Figure S**) and WB-BSG (**Figure S*18***).

	H-BSG (Figure S)		**WB-BSG (Figure S*18*)**	
% atomic concentration	**Map A**	**Map B**	**Map A**	**Map B**
Carbon	52.145	39.897	52.736	52.671
Oxygen	7.765	6.321	19.111	22.625
Nitrogen	39.054	42.204	27.777	24.422
Silicon	0.695	11.260	0.048	-
Nickel	0.166	0.269	0.116	0.070
Sulphur	0.174	0.049	0.212	0.213

1.2.11 Adsorption with $CdSO_4$

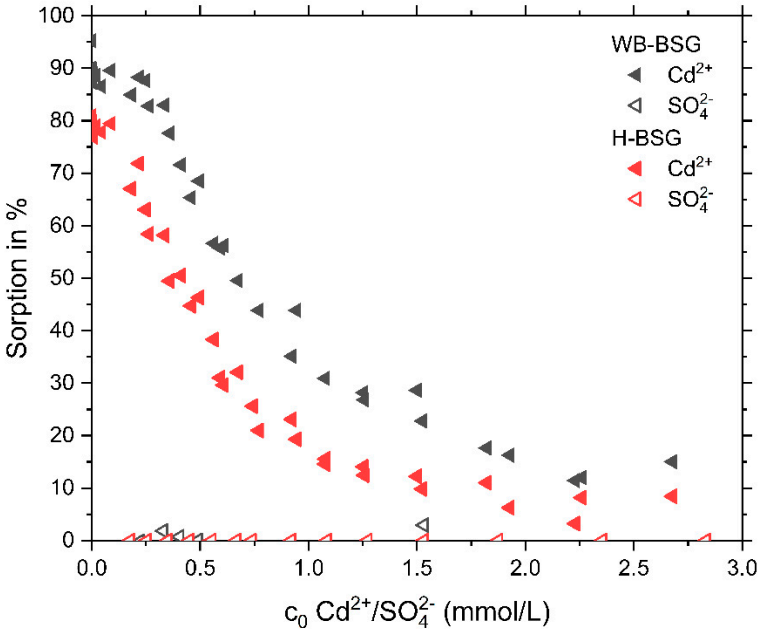

Figure S21. Adsorption in % for Cd^{2+} and SO_4^{2-} ions with H-BSG and WB-BSG, obtained from batch experiments and stirred for 24 h.

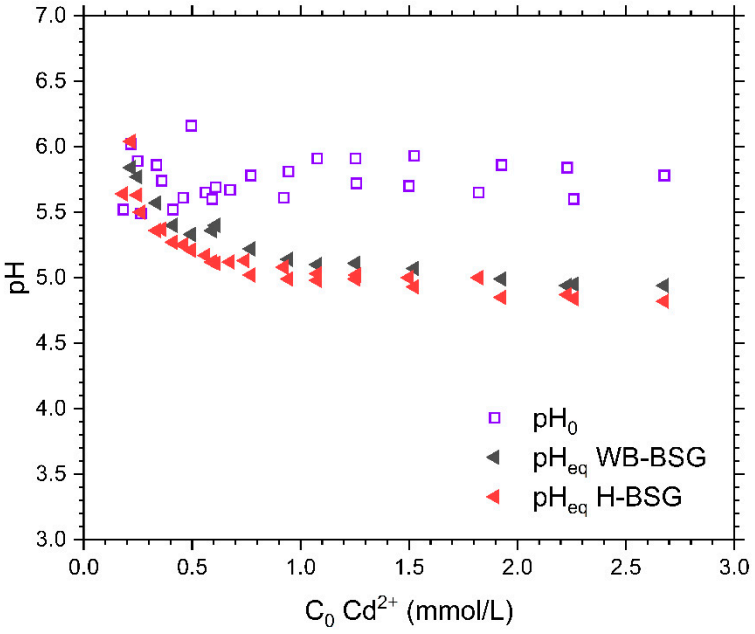

Figure S22. pH values before (pH_0) and after (pH_{eq}) for the adsorption of Cd^{2+} and SO_4^{2-} ions onto H-BSG and WB-BSG, obtained from batch experiments, stirred 24 h and pH not adjusted.

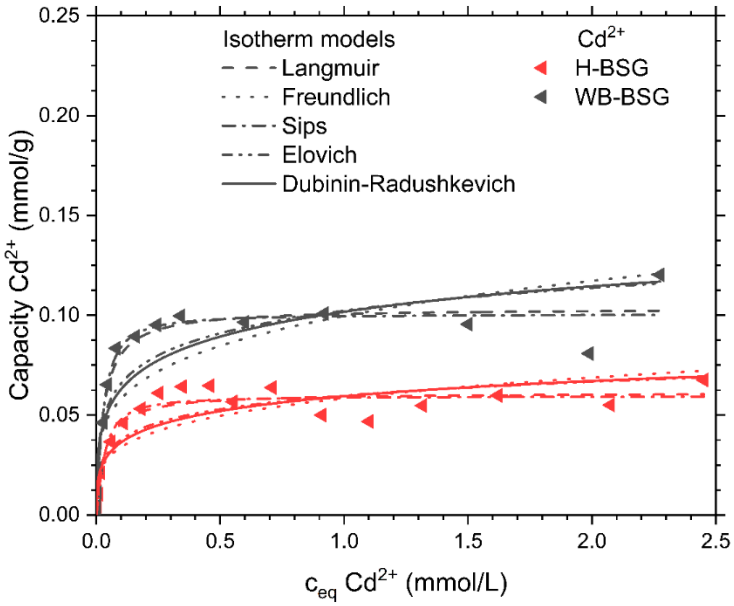

Figure S23. Curve fitting of different isotherm models onto Cd^{2+} ion adsorption onto H-BSG (red) and WB-BSG (grey) in batch experiment. Isotherm model fitting for $CdSO_4$ and $NiSO_4$

Table S12. Comparison fitting parameters for different adsorption isotherm models, values for Figure S18 and Figure **S23**.

Adsorption parameters	**Ni^{2+}**		**Cd^{2+}**	
	H-BSG	**WB-BSG**	**H-BSG**	**WB-BSG**
Langmuir				
$Q_{m,L}$ (mmol/g)	0.048±0.001	0.095±0.004	0.061±0.002	0.104±0.003
K_L (L/mmol)	15.889±2.587	4.017±0.508	29.228±6.406	34.638±5.947
R^2	0.969	0.977	0.966	0.976
ΔG° (kJ/mol)	-8.306	-8.724	-6.806	-3.422
Freundlich				
n	4.777±0.849	2.930±2.929	4.238±0.696	4.263±0.681
K_F (L/mmol)$^{1/n}$	0.045±0.002	0.073±0.002	0.058±0.003	0.100±0.007
R^2	0.837	0.943	0.833	0.843
Sips				
$Q_{m,S}$ (mmol/g)	0.0476±0.002	0.104±0.011	0.0595±0.002	0.101±0.003
K_S (L/mmol)^n	20.984±11.856	2.730±1.038	78.559±72.000	92.796±73.421
n	1.098±0.185	0.849±0.132	1.280±0.246	1.262±0.206
R^2	0.9670	0.979	0.969	0.979
Elovich				
$Q_{m,E}$ (mmol/g)	0.009 ±0,001	0.030 ± 0.003	0.012 ± 0.002	0.020 ± 0.003
K_E	644.423±543.065	30.079±9.951	751.719±600.500	963.399±722.492
R^2	0.908	0.972	0.908	0.922
Dubinin-Radushkevich				
$Q_{m,DR}$ (mmol/g)	0.084 ± 0.010	0.215 ± 0.021	0.112 ± 0.013	0.189 ± 0.022
β (10^{-9} mol^2/J^2)	2.087 ± 0.319	3.632 ± 0.291	2.165 ± 0.326	2.110 ± 0.300
R^2	0.889	0.963	0.882	0.894
$E_{Ads,DR}$	15.48 ± 1.18	11.73 ± 0.47	15.20 ± 1.14	15.39 ± 1.10

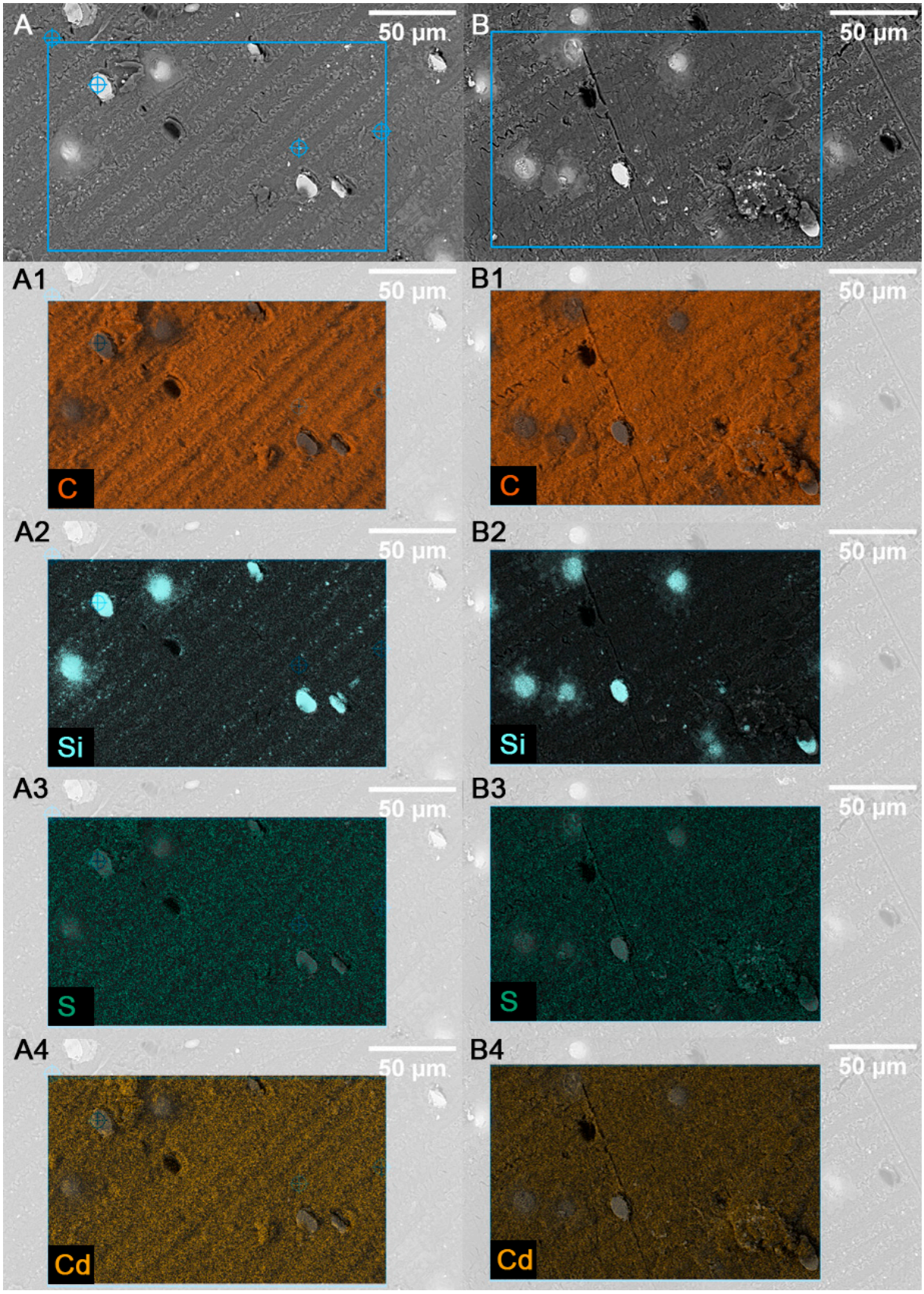
A
50 µm
B
50 µm
A1
50 µm
C
B1
50 µm
C
A2
50 µm
Si
B2
50 µm
Si
A3
50 µm
S
B3
50 µm
S
A4
50 µm
Cd
B4
50 µm
Cd

Figure S24. SEM-EDX elemental mapping of H-BSG after adsorption in batch experiments with $CdSO_4$ (2.7 mmol/L), 24 h at 23 °C, universal scale bars = 50 µm. Subfigures A and B are SEM micrographs of mapped areas. Subfigures show selected element mappings: A1 and B1 carbon; A2 and B2 silicon; A3 and B3 sulphur and A4 and B4 cadmium.

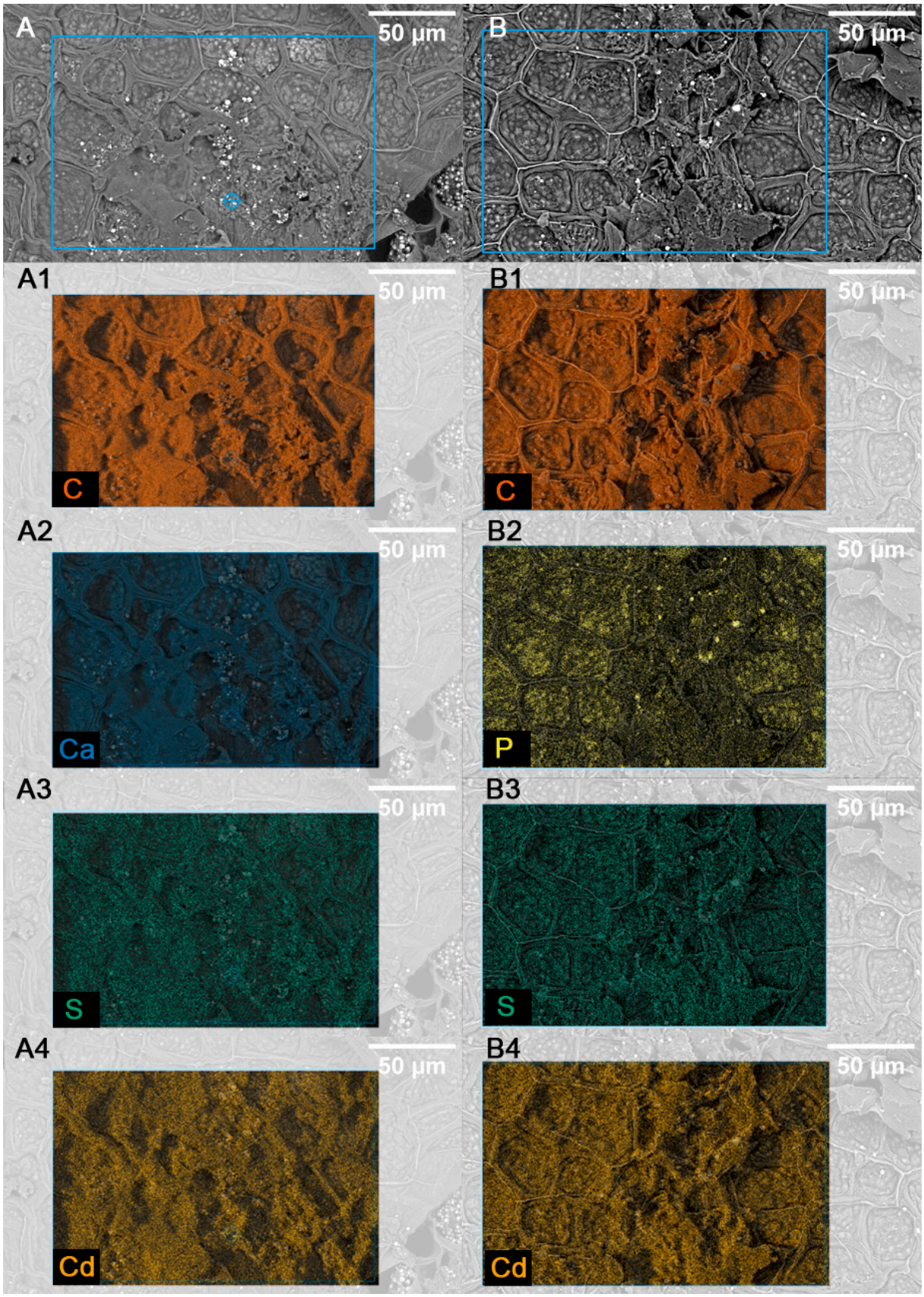

Figure S25. SEM-EDX elemental mapping of WB-BSG after adsorption in batch experiments with $CdSO_4$ (2.7 mmol/L), 24 h at 23 °C, universal scale bars = 50 μm. Subfigures A and B are SEM micrographs of mapped areas. Subfigures show selected element mappings: A1 and B1 carbon; A2 calcium and B2 phosphorus; A3 and B3 sulphur and A4 and B4 cadmium.

Table S13. Elemental concentration as percentages detected on BSG surface after adsorption in batch experiments with $CdSO_4$ (H-BSG: 2.7 mmol/L; WB-BSG 2.7 mmol/L), 24 h at 23 °C. Investigated in two areas (map A and map B) of H-BSG (***Figure S20***) and WB-BSG (***Figure S21***).

	H-BSG (Figure S20)		**WB-BSG (Figure S21)**	
% atomic concentration	**Map A**	**Map B**	**Map A**	**Map B**
Carbon	58.188	61.624	54.644	59.305
Oxygen	8.981	4.713	15.448	10.030
Nitrogen	31.711	32.414	28.799	29.878
Phosphorus	-	-	0.496	0.400
Calcium	-	-	0.139	-
Silicon	0.974	1.028	-	-
Cadmium	0.061	0.135	0.286	0.257
Sulphur	0.085	0.086	0.131	0.129

2 Literature comparison of adsorption capacities

2.1 Literature comparison of adsorption capacities for iron ions

Table S144. Sorption capacities for $Fe^{2+/3+}$ removal from aqueous solutions with different biosorbents and adsorbent doses (a.d.). The obtained sorption capacities from this work were achieved in the batch adsorption experiments.

Material	Sorption capacity q (mg/g)	Salt	Experimental conditions			Ref.
			pH_0	a.d. (g/L)	t, T	
***Helles* brewer's spent grain**	10.2	$FeSO_4$	5.5	3.33	24 h, 23 °C	This work
Wheat beer brewer's spent grain	11.7	$FeSO_4$	5.5	3.33	24 h, 23 °C	This work
brewer's spent grain	4 ± 1	$FeSO_4$	5.9	2	24 h, 21 °C	[4]
brewer's spent grain	8.33	$FeCl_3$	8	20	2 h,	[2]
brewer's spent grain (Sorghum)	1.77	$FeSO_4$	5	5	10 h, 30 °C	[5]
Chitosan	128.8	$FeSO_4$	-	3.33	24 h, RT	[7]
C. vulgaris (algea)	74.54	$FeSO_4$	6	0.4	5 h, 25 °C	[8]
activated carbon from coconut shell	58.76	$FeSO_4$	5.8	0.2	2 h, 25 °C	[9]
cow bone charcoal	31.43	$FeSO_4$	5.1	0.2	110 min, 25 °C	[10]

2.2 Literature comparison of adsorption capacities for manganese ions

Table S1515. Sorption capacities for $Mn^{1+/2+}$ removal from aqueous solutions with different biosorbents and adsorbent doses (a.d.). The obtained sorption capacities from this work were achieved in the batch adsorption experiments.

Material	Sorption capacity q (mg/g)	Salt	Experimental conditions			Ref.
			pH_0	a.d. (g/L)	t, T	
***Helles* brewer's spent grain**	3.72	$MnSO_4$	6	3.33	24 h, 22 °C	This work
Wheat beer brewer's spent grain	5.71	$MnSO_4$	6	3.33	24 h, 22 °C	This work
brewer's spent grain	0.96 ± 0.02	$MnSO_4$	-	2.0	24 h, 21 °C	[4]
brewer's spent grain	1.1	Mn (II)	4.4-4.5	2.5	1 h,-	[11]
Sugarcane bagasse	0.676	$MnSO_4$	4.5	15	1 h, 23 ± 2 °C	[12]
Chitosan	27.5	$MnSO_4$	-	3.33	24 h, RT	[7]
Pecan nutshell	98.0	$MnSO_4$	-	5.5	5 h, 25 °C	[13]
***Arthrobacter* cells**	406	Mn (II)	5-5.5	0.26	30 °C	[14]
C. vulgaris (algea)	69.29	$MnCl_2$	6	0.4	5 h, 25 °C	[8]
hydrolyzed olive cake	3.57	$MnNO_3$	6	5	2 h, 25 °C	[15]
volcanic ash geopolymer	192	$MnSO_4$	6.3	5	30 min, RT	[16]
metakaolin based geopolymer	72.34	$MnSO_4$	6	3.2	25 min, 30 °C	[17]
activated carbon from coconut shell	51.23	$Mn(NO_3)_2$	5.8	0.2	2 h, 25 °C	[9]
cow bone charcoal	29.59	$Mn(NO_3)_2$	5.1	0.2	110 min, 25 °C	[10]
sodium alginate/graphene oxide double network hydrogel	56.49	$MnCl_2$	6	3	9 h, 25 °C	[18]

2.3 Literatur comparison of adsorption capacities for nickel ions

Table S16. Sorption capacities for Ni^{2+} removal from aqueous solutions with different biosorbents and adsorbent doses (a.d.). The obtained sorption capacities from this work were achieved in the batch adsorption experiments.

Material	Sorption capacity q (mg/g)	Salt	Experimental conditions			Ref.
			pH_0	a.d. (g/L)	t, T	
Helles brewer's spent grain	2.79	$NiSO_4$	6	3.33	24 h, 23 °C	This work
Wheat beer brewer's spent grain	6.10	$NiSO_4$	6	3.33	24 h, 23 °C	This work
peat	0.23	$Ni(NO_3)$	-	0.8	24 h, RT	[6]
chitosan	105.6	$NiSO_4$	5.4	2	24 h, RT	[7]
poly(vinylpyrrolidone) hydrogel	13.43	$NiCl_2$	8	1	6 h, 25 °C	[19]
poly(vinylpyrrolidone-comethylacrylate) hydrogel	71.52	$NiCl_2$	8	1	6 h, 25 °C	[19]
activated carbon from coconut shell	67.56	$Ni(NO_3)_2$	5.8	0.2	2 h, 25 °C	[9]
Cow bone charcoal	32.54	$Ni(NO_3)_2$	5.1	0.2	110 min, 25 °C	[10]
chitosan	66.3	$Ni(NO_3)_2$	-	1	5 d, 30 °C	[20]
chitosan	49.89	$NiSO_4$	-	1	5 d, 30 °C	[20]

2.4 Literatur comparison of adsorption capacities for cadmium ions

Table S17. *Sorption capacities for Cd^{2+} removal from aqueous solutions with different biosorbents and adsorbent doses (a.d.). The obtained sorption capacities from this work were achieved in the batch adsorption experiments.*

Material	Sorption capacity q (mg/g)	Salt	Experimental conditions			Ref.
			pH_0	a.d. (g/L)	t, T	
Helles brewer's spent grain	6.61	$CdSO_4 \cdot H_2O$	5,5	3,33	24 h, 23 °C	This work
Wheat beer brewer's spent grain	11.40	$CdSO_4 \cdot H_2O$	5,5	3,33	24 h, 25 °C	This work
H-Ch60-2	195.6	$CdSO_4 \cdot H_2O$	5.5	3.33	24 h, 25 °C	[21]
Oxidized potato starch	7.9	$CdSO_4 \cdot H_2O$	6.1	2	2 h, 25 °C	[22]
Oxidized corn starch	7.7	$CdSO_4 \cdot H_2O$	6.1	2	2 h, 25 °C	[22]
Native potato starch	1.6	$CdSO_4 \cdot H_2O$	6.1	2	2 h, 25 °C	[22]
Aminopyridine modified poly(styrene-alt-maleic anhydride)	81.30	$CdSO_4 \cdot H_2O$	5	2.5	60 min, 25 °C	[23]
Ficus religiosa Leaf Powder	27.14	$CdSO_4 \cdot 8H_2O$	5	-	30 min, 30 °C	[24]
Carbon prepared from apricot stone	33.57	$CdSO_4 \cdot 8H_2O$	6	2	48 h, 25 °C	[25]
Biomass xanthates	19.6	$CdCl_2$	6 - 8	0.20	2 h, 20 °C	[26]
Graphene oxide / starch composite	29.04	n.a.	n.a.	2.5	2 h, 25 °C	[27]
Crosslinked carboxymethyl starch (CCS)	47	$CdCl_2$	6	50	1 h, 25 °C	[27]
Chitosan-thiourea hydrogel	156	$CdSO_4$	5.6	0.5	24 h, 25 °C	[28]
Chitosan	160	$CdCl_2$	7	1	24 h, 25 °C	[29]
Chitosan-based hydrogel	234.83	$Cd(NO_3)_2$	6.0	2	24 h, 40 °C	[30]
Activated carbon/ Fe/ chitosan hybrid	344	$Cd(NO_3)_2$	6.0	10	24 h, 25 °C	[31]

3 References

1. Su, Y.; Böhm, W.; Wenzel, M.; Paasch, S.; Acker, M.; Doert, T.e.a. Mild hydrothermally treated brewer's spent grain for efficient removal of uranyl and rare earth metal ions. *RSC Advances* **2020**, *10*, 45116–45129, doi:10.1039/D0RA08164G.
2. Izinyon, O.C.; Nwosu, O.E.; Lo Akhigbe; Ilaboya, I.R. Performance Evaluation of Fe (III) Adsorption onto Brewers' Spent Grain. *Nigerian Journal of Technology* **2016**, *35*, S. 970–978, doi:10.4314/njt.v35i4.36.
3. Khidzir K.M; Noorlidah Abdullah; Agamuthu P. Brewery Spent Grain: Chemical Characteristics and utilization as an Enzyme Substrate. *Malaysian Journal of Science* **2010**, *29*, S. 41–51, doi:10.22452/mjs.vol29no1.7.
4. Fontana, I.B.; Peterson, M.; Cechinel, M.A.P. Application of brewing waste as biosorbent for the removal of metallic ions present in groundwater and surface waters from coal regions. *Journal of Environmental Chemical Engineering* **2018**, *6*, 660–670, doi:10.1016/j.jece.2018.01.005.
5. Akinpelu, E.A.; Fosso-Kankeu, E.; Waander, F. Biosorption of Fe (II) from aqueous solution by brewing waste: Equilibrium and kinetic studies. *Journal of Water and Environment Technology 17* **2019**, S. 180–193, doi:10.2965/jwet.18-081.
6. Charazińska, S.; Lochyński, P.; Burszta-Adamiak, E. Removal of heavy metal ions form acidic electrolyte for stainless steel electropolishing via adsorption using Polish peats. *Journal of Water Process Engineering* **2021**, *42*, 102169, doi:10.1016/j.jwpe.2021.102169.
7. Weißpflog, J.; Gündel, A.; Vehlow, D.; Steinbach, C.; Müller, M.; Boldt, R.e.a. Solubility and Selectivity Effects of the Anion on the Adsorption of Different Heavy Metal Ions onto Chitosan. *Molecules (Basel, Switzerland)* **2020**, doi:10.3390/molecules25112482.
8. Ahmad, A.; Bhat, A.H.; Buang, A. Biosorption of transition metals by freely suspended and Ca-alginate immobilised with Chlorella vulgaris: Kinetic and equilibrium modeling. *Journal of Cleaner Production* **2018**, 1361–1375, doi:10.1016/j.jclepro.2017.09.252.
9. Moreno-Piraján, J.C.; Garcia-Cuello, V.S.; Giraldo, L. The removal and kinetic study of Mn, Fe, Ni and Cu ions from wastewater onto activated carbon from coconut shells. *Adsorption* **2010**, 505–514, doi:10.1007/s10450-010-9311-5.

10. Moreno, J.C.; Gómez, R.; Giraldo, L. Removal of Mn, Fe, Ni and Cu Ions from Wastewater Using Cow Bone Charcoal. *Materials* **2010**, 452–466, doi:10.3390/ma3010452.
11. Wierzba, S.; Kłos, A. Heavy metal sorption in biosorbents – Using spent grain from the brewing industry. *Journal of Cleaner Production* **2019**, *225*, 112–120, doi:10.1016/j.jclepro.2019.03.286.
12. Esfandiar, N.; Nasernejad, B.; Ebadi, T. Removal of Mn(II) from groundwater by sugarcane bagasse and activated carbon (a comparative study): Application of response surface methodology (RSM). *Journal of Industrial and Engineering Chemistry* **2014**, *20*, 3726–3736, doi:10.1016/j.jiec.2013.12.072.
13. Vaghetti, J.C.P.; Lima, E.C.; Royer, B.; Da Cunha, B.M.; Cardoso, N.F.; Brasil, J.L.; Dias, S.L.P. Pecan nutshell as biosorbent to remove Cu(II), Mn(II) and Pb(II) from aqueous solutions. *Journal of hazardous materials* **2009**, *162*, 270–280, doi:10.1016/j.jhazmat.2008.05.039.
14. Veglió, F.; Beolchini, F.; Gasbarro, A. Biosorption of toxic metals: an equilibrium study using free cells of Arthrobacter sp. *Process Biochemistry* **1997**, *32*, 99–105, doi:10.1016/S0032-9592(96)00047-7.
15. Fernández-González, R.; Martín-Lara, M.A.; láñez-Rodríguez, I.; Calero, M. Removal of heavy metals from acid mining effluents by hydrolyzed olive cake. *Bioresource Technology* **2018**, *268*, 169–175, doi:10.1016/j.biortech.2018.07.124.
16. Anguile, J.J.; Ona-Mbega, M.; Makani, T.; Ketcha-Mbadcam, J. Adsorption of manganese (II) ions from aqueous solution on to volcanic ash and geopolymer based volcanic ash. *International Journal of Basic and Applied Chemical Sciences* **2013**, 7–18.
17. Kara, I.; Tunc, D.; Sayin, F.; Akar, S.T. Study on the performance of metakaolin based geopolymer for Mn(II) and Co(II) removal. *Applied Clay Science* **2018**, 184–193, doi:10.1016/j.clay.2018.04.027.
18. Yang, X.; Zhou, T.; Ren, B.; Hursthouse, A.; Zhang, Y. Removal of Mn (II) by Sodium Alginate/Graphene Oxide Composite Double-Network Hydrogel Beads from Aqueous Solutions. *Sci Rep* **2018**, 10717, doi:10.1038/s41598-018-29133-y.
19. Kemik, Ö.; Ngwabebhoh, F.A.; Yildiz, U. A response surface modelling study for sorption of Cu2+, Ni2+, Zn2+ and Cd2+ using chemically modified poly(vinylpyrrolidone) and poly(vinylpyrrolidone-co-methylacrylate) hydrogels.

Adsorption Science & Technology **2016**, 263–283, doi:10.1177/0263617416674950.

20. Wu, F.-C.; Tseng, R.-L.; Juang, R.-S. A review and experimental verification of using chitosan and its derivatives as adsorbents for selected heavy metals. *Journal of Environmental Management* **2010**, 798–806.
21. Reis, B.; Gerlach, N.; Steinbach, C.; Haro Carrasco, K.; Oelmann, M.; Schwarz S.; Müller, M.; Schwarz D. A Complementery und Revised View on the N-Acylation of Chitosan with Hexanoyl Chloride. *Marine Drugs* **2021**, doi:10.3390/md19070385.
22. Borchert, K.; Boughanmi, R.; Reis, B.; Zimmermann, P.; Steinbach, C.; Graichen, P.; Svirepa, A.; Schwarz, J.; Boldt, R.; Schwarz, S.; et al. Removal of Lead, Cadmium, and Aluminum Sulfate from Simulated and Real Water with Native and Oxidized Starches. *Polysaccharides* **2021**, 429–453, doi:10.3390/polysaccharides2020027.
23. Rao, K.S.; Anand, S.; Venkateswarlu, P. Adsorption of Cadmium from Aqueous Solution by Ficus religiosa Leaf Powder and Characterization of Loaded Biosorbent. *Clean Soil Air Water* **2011**, 384–391, doi:10.1002/clen.201000098.
24. Kobya, M.; Demirbas, E.; Senturk, E.; Ince, M. Adsorption of heavy metal ions from aqueous solutions by activated carbon prepared from apricot stone. *Bioresour. Technol* **2005**, 1518–1521, doi:10.1016/j.biortech.2004.12.005.
25. Li, W.; Liao, X.; Wang, L.; Huang, Z. Adsorption of cadmium and lead in wastewater by four kinds of biomass xanthates. *Water Sci. Technol* **2019**, 1222–1230, doi:10.2166/wst.2019.124.
26. Wang, Z.; Zhang, X.; Wu, X.; Yu, J.-G.; Jiang, X.-Y.; Wu, Z.-L.; Hao, X. Soluble starch functionalized graphene oxide as an efficient adsorbent for aqueous removal of Cd(II): The adsorption thermodynamic, kinetics and isotherms. *J Sol-Gel Sci Technol* **2017**, 440–449, doi:10.1007/s10971-017-4313-3.
27. Chen, Y.X.; Zhong, B.H.; Fang, W. Adsorption characterization of lead(II) and cadmium(II) on crosslinked carboxymethyl starch. *J. Appl. Polym. Sci.* **2011**, 5010–5020, doi:10.1002/app.35607.
28. Ghiorghita, C.-A.; Borchert, K.; Vasiliu, A.-L.; Zaharia, M.-M.; Schwarz, D.; Mihai, M. Porous thiourea-grafted-chitosan hydrogels: Synthesis and sorption of toxic metal ions from contaminated waters. *Colloids and Surfaces A: Physicochemical and Engineering Aspects* **2020**, 125504, doi:10.1016/j.colsurfa.2020.125504.

29. Dzul Erosa, M.S.; Saucedo Medina, T.I.; Navarro Mendoza, R.; Avila Rodriguez, M.; Guibal, E. Cadmium sorption on chitosan sorbents: kinetic and equilibrium studies. *Hydrometallurgy* **2001**, 157–167, doi:10.1016/S0304-386X(01)00166-9.
30. Vilela, P.; Matias, C.; Dalalibera, A.; Becegato, V.; Paulino, A. Polyacrylic Acid-Based And Chitosan-Based Hydrogels For Adsorption Of Cadmium: Equilibrium Isotherm, Kinetic And Thermodynamic Studies. *Journal of Environmental Chemical Engineering* **2019**, 103327, doi:10.1016/j.jece.2019.103327.
31. Sharififard, H.; Shahraki, Z.; Rezvanpanah, E.; Rad, S. A Novel Natural Chitosan/Activated Carbon/Iron Bio-Nanocomposite: Sonochemical Synthesis, Characterization, And Application For Cadmium Removal In Batch And Continuous Adsorption Process. *Bioresource Technology* **2018**, 562–569, doi:10.1016/j.biortech.2018.09.094.